

Impact of carbon and nitrogen impurities in high- κ dielectrics on metal-oxide-semiconductor devices

Minseok Choi,^{a)} John L. Lyons, Anderson Janotti, and Chris G. Van de Walle
 Materials Department, University of California, Santa Barbara, California 93106, USA

(Received 3 December 2012; accepted 28 March 2013; published online 8 April 2013)

We investigate the electronic structure of carbon and nitrogen impurities, which are commonly incorporated during atomic-layer deposition of high- κ oxides such as Al_2O_3 and HfO_2 . The impact on metal-oxide-semiconductor devices is assessed by examining formation energies, transition levels, and band alignment between the oxide and semiconductors such as GaN, Si, and III-As. Carbon introduces charge-state transition levels near the semiconductor conduction-band edges, resulting in border traps and/or leakage current. Nitrogen acts as a source of negative fixed charge but may also be effective in alleviating the problem of carrier traps associated with native defects.

© 2013 AIP Publishing LLC. [<http://dx.doi.org/10.1063/1.4801497>]

The use of high- κ gate oxides such as HfO_2 in silicon metal-oxide-semiconductor (MOS) devices has attracted considerable attention due to requirements in device scaling.¹ Concurrently, oxide/III-V MOS structures have been intensively investigated, with the potential of adding flexibility to device design and functionalities in MOS electronics. The oxides are typically deposited by atomic layer deposition (ALD), and promising results have been achieved with Al_2O_3 /III-V, exhibiting relatively low interface-state densities in MOS structures.^{2,3}

The carrier traps and fixed charges that are observed are commonly attributed to intrinsic point defects in the oxide dielectrics, located at or near the interface.^{3–5} However, there is solid evidence for the presence of significant concentrations of impurities in oxides grown by ALD, and the impact of those impurities on electronic performance has received far less attention to date. The use of metal-organic precursors and low-temperature growth conditions often results in incomplete decomposition of precursors and residual concentrations of carbon or nitrogen impurities in the oxide layer.^{6,7} Incorporation of up to 0.2 at. % of carbon⁸ and ~5 at. % of nitrogen⁹ has been found in Al_2O_3 . In HfO_2 , concentrations of $\sim 10^{21} \text{ cm}^{-3}$ for C and $\sim 10^{20} \text{ cm}^{-3}$ for N have been reported.¹⁰

Carbon has been suggested as a cause of leakage current in HfO_2 /Si MOS structures, since leakage current correlates with carbon concentration in the HfO_2 layer.^{11,12} Nitrogen, on the other hand, has been found to lower the density of interface states and improve dielectric strength.^{13–15} The role of impurities in the electrical properties of Al_2O_3 has not been well explored.

In this letter, we report first-principles calculations based on density functional theory for carbon and nitrogen impurities in HfO_2 and Al_2O_3 . The few computational studies that were performed in the past were either incomplete or suffered from shortcomings in the methodology. Sankaran *et al.*¹⁶ reported G_0W_0 results for electronic states of C and N in $\gamma\text{-Al}_2\text{O}_3$ but limited their investigation to the neutral charge state. For HfO_2 , the prior calculations for C (Ref. 12) and for N (Refs. 17 and 18) all employed traditional density

functionals such as the local density approximation (LDA) or generalized gradient approximation (GGA), which suffer from a significant underestimation of the band gap, thus rendering it difficult to derive results for defect levels.

The use of a hybrid functional within density functional theory allows for an accurate description of band gaps, thereby enabling the prediction of impurity levels with respect to the band edges. We use the screened hybrid functional of Heyd-Scuseria-Ernzerhof (HSE),¹⁹ implemented with the projector augmented-wave method²⁰ in the *VASP* code.²¹ The HSE mixing parameter was set to 32%, resulting in band gaps of 9.2 eV for $\alpha\text{-Al}_2\text{O}_3$ and 5.8 eV for monoclinic HfO_2 . The electronic wave functions were expanded in a plane-wave basis set with an energy cutoff of 400 eV. Impurity calculations were performed using periodic boundary conditions with supercells containing 120 atoms for $\alpha\text{-Al}_2\text{O}_3$ and 96 atoms for monoclinic HfO_2 , and the integrations over the Brillouin zone were performed using a $2 \times 2 \times 1$ and k -point grid for Al_2O_3 and $2 \times 2 \times 2$ for HfO_2 .

The formation energy of an impurity X in charge state q is given by²²

$$E^f(X^q) = E_{\text{tot}}(X^q) - E_{\text{tot}}(\text{oxide}) - \sum_i n_i(\mu_i^0 + \mu_i) + q\epsilon_F + \Delta^q, \quad (1)$$

where $E_{\text{tot}}(X^q)$ is the total energy of a supercell containing the impurity X in charge state q , and $E_{\text{tot}}(\text{oxide})$ is the total energy of the bulk oxide in the same supercell. We investigate both substitutional (X_{Al} , X_{Hf} , and X_{O}) and interstitial configurations (X_i). In HfO_2 , two types of X_{O} exist: threefold-coordinated $X_{\text{O}3}$ and fourfold coordinated $X_{\text{O}4}$. n_i is the number of atoms of type i added to or removed from the perfect crystal, and μ_i is the atomic chemical potential. $\mu_{\text{Al(Hf)}}$ is referenced to the total energy per atom in bulk Al (Hf) metal [$\mu_{\text{Al(Hf)}}^0 = E_{\text{tot}}(\text{Al(Hf)})$], and μ_{O} is referenced to the total energy per atom of an isolated O_2 molecule [$\mu_{\text{O}}^0 = (1/2)E_{\text{tot}}(\text{O}_2)$]. Chemical potentials for the impurities are referenced to the energy per atom of diamond for C and the N_2 molecule for N. ϵ_F is the Fermi level referenced to the valence-band maximum (VBM), and Δ^q is the correction

^{a)}Electronic address: minseok@engineering.ucsb.edu

term to align the electrostatic potentials of the bulk and defect supercells and to account for finite-cell size effects on the total energies of charged defects.²³

Figure 1 shows the calculated formation energies of C and N in Al_2O_3 and HfO_2 as a function of Fermi level. For each Fermi level, only the formation energy of the charge state with lowest energy is shown. The Fermi-level positions where the charge state changes from q to q' correspond to transition levels (q/q'). Formation energies depend on chemical potentials, which in turn depend on growth conditions. A reasonable choice for ALD growth conditions is to set $\mu_{\text{O}} = -0.65$ eV, corresponding to contact with O_2 gas at 270°C and 1 Torr. Chemical potentials for Hf and Al are obtained by assuming equilibrium with HfO_2 and Al_2O_3 . Choice of precursors, presence of other gases, and deposition temperature may all affect the precise value. Non-equilibrium deposition conditions may also allow higher impurity concentrations in ALD oxides (as evidenced by experiment) than those that would correspond to our calculated formation energies. Figure 1 (in which μ_{O} is chosen at -0.65 eV) clearly shows, however, that for most Fermi-level positions carbon strongly prefers to occupy the cation sites both in Al_2O_3 and HfO_2 , and this finding is not sensitive to the precise value of the oxygen chemical potential.

We note that if dissociation of a carbon-including radical from the metal (Al or Hf) is a limiting factor, incorporation of C on an O site may seem more likely—in spite of the

high formation energy of C_{O} . However, there is strong evidence that metal-C bonds are weakened by interactions between the metal precursor and the surface. Al-C bonds in trimethylaluminum (TMA) have been reported to be weakened by Al-Al interactions on the surface during Al_2O_3 deposition, with a resulting activation energy for methyl-radical production of 0.56 eV.²⁴ For ALD of HfO_2 using tetrakis(ethylmethylamido)hafnium (TEMAH), the surface interactions have been reported to give an energy for CH_4 radical production of 0.17 eV.²⁵ Such low activation energies indicate that decomposition is not a bottleneck, and incorporation of carbon will be more likely on the site on which it has the lowest formation energy (which is the cation site, according to our calculations).

We also note that the charge-state transition levels (represented as kinks in Fig. 1), which determine the electrical activity of the impurity, are not affected by the choice of chemical potentials. The (+1/0) impurity level of C_{Al} occurs at 4.67 eV and the (0/−1) level at 6.17 eV above the VBM in Al_2O_3 . Hence, C_{Al} occurs in a positive charge state for $\epsilon_F < (+1/0)$ and a negative charge state when $\epsilon_F > (0/-1)$. In HfO_2 , C_{Hf} exhibits only one transition level, the (0/−1) level at 4.64 eV. C_{Hf} is, therefore, electrically inactive for most Fermi levels in HfO_2 .

For nitrogen, the results are more sensitive to chemical potentials. In Al_2O_3 , nitrogen interstitials are unfavorable, but the substitutional configurations are close in energy, with some preference for N_{O} . The (0/−1) level of the latter occurs at 3.21 eV above the VBM, hence N_{O} will be in a negative charge state for most relevant Fermi-level positions—a conclusion that actually holds for the other configurations of N in Al_2O_3 as well. In HfO_2 , all configurations of N have similar formation energies, and ultimately kinetics may determine which one is more likely to occur. But again, all these configurations will tend to be stable in the −1 charge state for the relevant Fermi-level positions.

In order to examine the impact of C and N on MOS devices, we need to align the band structure and impurity levels in the oxides with the semiconductor band edges. Figure 2 shows alignments based on band offsets taken from Refs. 5, 26, and 27. We will discuss oxides on GaN, Si, and III-arsenides separately; however, our conclusions (which will be that C acts as a carrier trap and N as a fixed-charge center) will turn out to be generally applicable.

Looking first at GaN-oxide structures, as noted above C_{Al} is the most likely configuration for C in Al_2O_3 . Its (+1/0) level occurs at 0.54 eV below the GaN conduction-band minimum (CBM), indicating that C in Al_2O_3 may act as a border trap in n -GaN-based MOS structures in which the Fermi level is near the GaN CBM. Likewise, if HfO_2 is used as the oxide, C_{Hf} introduces a (0/−1) level at 0.37 eV below the GaN CBM.

The nitrogen impurity levels for all N configurations in both oxides are positioned such that the impurity will be in a negative charge state for most Fermi-level positions below the midgap of GaN. Therefore, nitrogen acts as a source of negative fixed charge in the oxides.

Turning now to Si-based MOS structures, the carbon impurity favors the cation sites in both Al_2O_3 and HfO_2 and again introduces transition levels near the Si CBM. The C_{Al} (+1/0) level occurs at 0.13 eV below the Si CBM, and the

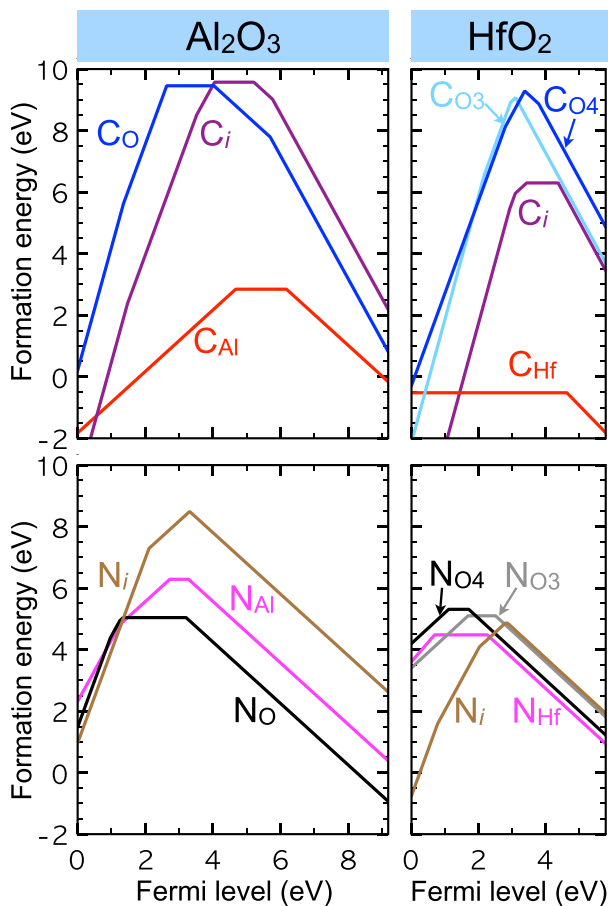


FIG. 1. Formation energies of C and N impurities in Al_2O_3 (left) and HfO_2 (right) for $\mu_{\text{O}} = -0.65$ eV. O3 and O4 are the threefold- and fourfold-coordinated oxygen sites.

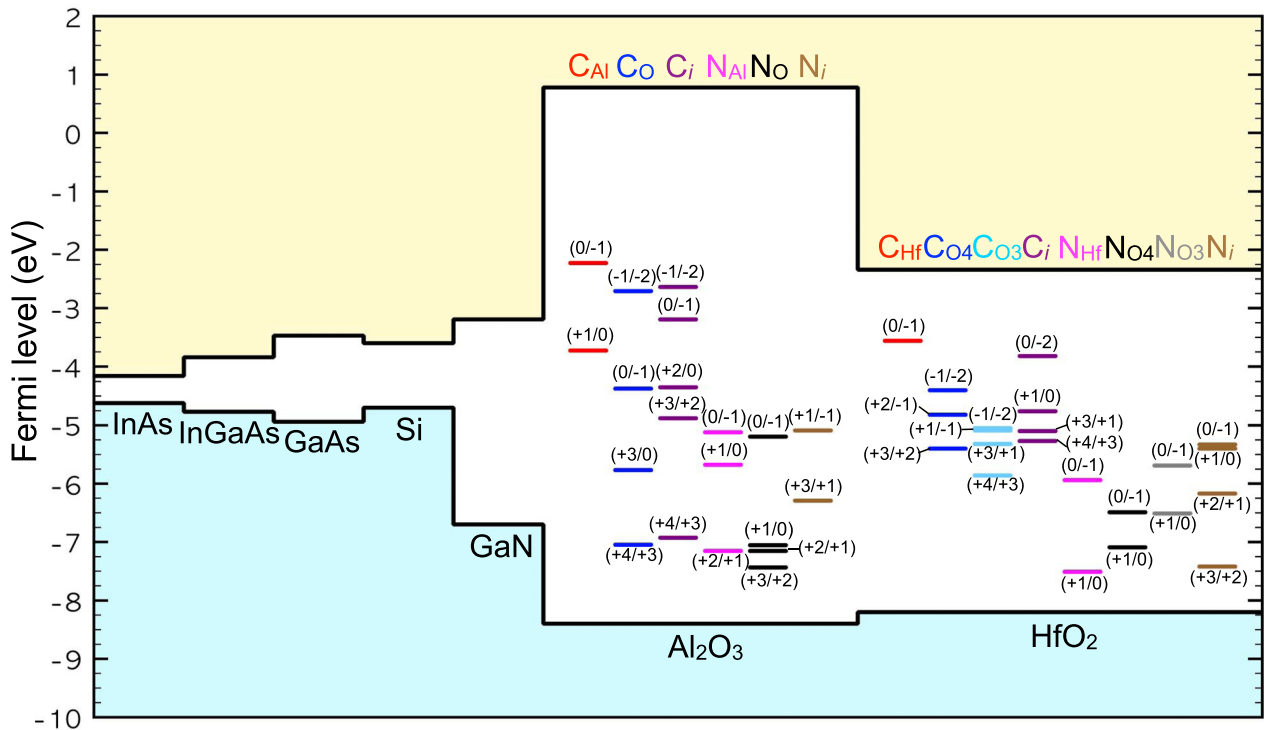


FIG. 2. Band alignment between semiconductors (III-As, Si, GaN) and oxide dielectrics (Al_2O_3 , HfO_2). The positions of charge-state transition levels for C and N impurities in Al_2O_3 and HfO_2 are shown within the oxide band gaps and relative to the semiconductor band edges. The zero was set at the vacuum level, with the GaN band-edge positions taken from Ref. 28.

C_{Hf} (0/−1) level at 0.04 eV above the Si CBM. These indicate that C leads to border traps and/or increased leakage current through the gate oxides, which is consistent with experimental observations on leakage-current differences between HfO_2 layers with different C content on top of Si.^{11,12}

As for nitrogen, it again leads to negative fixed charges since the transition levels occur more than ~ 2 eV below the Si CBM. Nitrogen may actually also have a beneficial role, in that it suppresses the formation of oxygen vacancies (which may have a tendency to form due to non-equilibrium ALD deposition conditions). Under oxygen-deficient conditions, N_O has a lower formation energy than oxygen vacancies and would thus reduce the concentration of vacancy-induced carrier traps. This is consistent with experiments that report improved electrical properties when N is incorporated in HfO_2/Si MOS structures.^{13–15}

The overall features of III-As-based MOS structures are very similar to the case of oxide/Si MOS structures. The (+1/0) level of C_{Al} and (0/−1) level of C_{Hf} occur near the CBM of InGaAs (0.11–0.28 eV above), and hence those impurities may act as a source of border traps and/or increase leakage current. All levels for nitrogen are again well below the InGaAs VBM, indicating it will act as a negative fixed-center.

To summarize, we have presented hybrid functional calculations for carbon and nitrogen impurities in Al_2O_3 and HfO_2 and the impact of these impurities on GaN, Si, and III-As semiconductor based MOS devices. We find that carbon incorporates preferentially on the cation site and produces carrier traps with an energy level near the semiconductor

CBM. Nitrogen acts as a source of negative fixed charge but may also help to reduce carrier traps due to native defects. Overall, our results call attention to the fact that incorporation of impurities (particularly carbon) is a concern in oxide dielectrics and should be more carefully controlled in order to achieve high-quality MOS devices.

We thank Professor P. McIntyre for useful discussions. M.C. was supported by the ONR DEFINE MURI (N00014-10-1-0937). J.L. was supported by the Semiconductor Research Corporation (Task No. 1867.001). A.J. was supported by the U. S. Army Research Office (W911-NF-11-1-0232). Computational resources were provided by the Center for Scientific Computing at the CNSI and MRL (an NSF MRSEC, DMR-1121053) (NSF CNS-0960316), and by XSEDE (NSF OCI-1053575).

¹G. He, L. Zhu, Z. Sun, Q. Wan, and L. Zhang, *Prog. Mater. Sci.* **56**, 475 (2011).

²Y. C. Chang, W. H. Chang, H. C. Chiu, L. T. Tung, C. H. Lee, K. H. Shiu, M. Hong, J. Kwo, J. M. Hong, and C. C. Tsai, *Appl. Phys. Lett.* **93**, 053504 (2008).

³N. Nepal, N. Y. Garces, D. J. Meyer, J. K. Hite, M. A. Mastro, and C. R. Eddy, Jr., *Appl. Phys. Express* **4**, 055802 (2011).

⁴B. Shin, J. R. Weber, R. D. Long, P. K. Hurley, C. G. V. de Walle, and P. C. McIntyre, *Appl. Phys. Lett.* **96**, 152908 (2010).

⁵J. R. Weber, A. Janotti, and C. G. Van de Walle, *J. Appl. Phys.* **109**, 033715 (2011).

⁶R. L. Puurunen, *J. Appl. Phys.* **97**, 121301 (2005).

⁷X. Liu, S. Ramanathan, A. Longdergan, A. Srivastava, E. Lee, T. Seidel, J. Barton, D. Pang, and R. Gordon, *J. Electrochem. Soc.* **152**, G213 (2005).

⁸K. Kukli, M. Ritala, M. Leskela, and J. Jokinen, *J. Vac. Sci. Technol. A* **15**, 2214 (1997).

⁹S. Lee and H. Jeon, *Electron. Mater. Lett.* **3**, 17 (2007).

- ¹⁰S. Kamiyama, T. Miura, and Y. Nara, *Appl. Phys. Lett.* **87**, 132904 (2005).
- ¹¹M. Cho, D. S. Jeong, J. Park, H. B. Park, S. W. Lee, T. J. Park, C. S. Hwang, G. H. Jang, and J. Jeong, *Appl. Phys. Lett.* **85**, 5953 (2004).
- ¹²M. Cho, J. H. Kim, C. S. Hwang, H.-S. Ahn, S. Han, and J. Y. Won, *Appl. Phys. Lett.* **90**, 182907 (2007).
- ¹³W. J. Maeng and H. Kim, *Appl. Phys. Lett.* **91**, 092901 (2007).
- ¹⁴H. Wong, B. Sen, B. L. Yang, A. P. Huang, and P. K. Chu, *J. Vac. Sci. Technol. B* **25**, 1853 (2007).
- ¹⁵J. H. Kim, T. J. Park, M. Cho, J. H. Jang, M. Seo, K. D. Na, C. S. Hwang, and J. Y. Won, *J. Electrochem. Soc.* **156**, G48 (2009).
- ¹⁶K. Sankaran, G. Pourtois, R. Degraeve, M. B. Zahid, G.-M. Rignanese, and J. V. Houdt, *Appl. Phys. Lett.* **97**, 212906 (2010).
- ¹⁷J. L. Gavartin, A. L. Shluger, A. S. Foster, and G. I. Bersuker, *J. Appl. Phys.* **97**, 053704 (2005).
- ¹⁸N. Umezawa, K. Shiraishi, Y. Akasaka, A. Oshiyama, S. Inumiya, S. Miyazaki, K. Ohmori, T. Chikyow, T. Ohno, K. Yamabe *et al.*, *Phys. Rev. B* **77**, 165130 (2008).
- ¹⁹J. Heyd, G. E. Scuseria, and M. Ernzerhof, *J. Chem. Phys.* **118**, 8207 (2003); A. V. Krukau, O. A. Vydrov, A. F. Izmaylov, and G. E. Scuseria, *ibid.* **125**, 224106 (2006).
- ²⁰P. E. Blöchl, *Phys. Rev. B* **50**, 17953 (1994).
- ²¹G. Kresse and J. Hafner, *Phys. Rev. B* **48**, 13115 (1993).
- ²²C. G. Van de Walle and J. Neugebauer, *J. Appl. Phys.* **95**, 3851 (2004).
- ²³C. Freysoldt, J. Neugebauer, and C. G. Van de Walle, *Phys. Rev. Lett.* **102**, 016402 (2009); *Phys. Status Solidi B* **248**, 1067 (2011).
- ²⁴D. W. Squire, C. S. Dulcey, and M. C. Lin, *J. Vac. Sci. Technol. B* **3**, 1513 (1985).
- ²⁵K. Li, S. Li, N. Li, T. M. Klein, and D. A. Dixon, *J. Phys. Chem. C* **115**, 18560 (2011).
- ²⁶J. L. Lyons, A. Janotti, and C. G. Van de Walle, *Microelectron. Eng.* **88**, 1452 (2011).
- ²⁷M. Choi, A. Janotti, and C. G. Van de Walle, *J. Appl. Phys.* **113**, 044501 (2013).
- ²⁸C. G. Van de Walle and J. Neugebauer, *Nature* **423**, 626 (2003).